Neurological Sciences (2021) 42:4271–4280
https://doi.org/10.1007/s10072-021-05380-2

ORIGINAL ARTICLE

# Novel biallelic mutations in *POLG* gene: large deletion and missense variant associated with PEO

Yan Lin[1] · Jixiang Du[1] · Wei Wang[1] · Hong Ren[1] · Dandan Zhao[1] · Fuchen Liu[1] · Pengfei Lin[1] · Kunqian Ji[1] · Yuying Zhao[1] · Chuanzhu Yan[1,2,3]

Received: 6 April 2021 / Accepted: 3 June 2021 / Published online: 29 June 2021


## Abstract

**Background** Mitochondrial disorders are clinically heterogeneous diseases associated with impaired oxidative phosphorylation (OXPHOS) activity. *POLG*, which encodes the DNA polymerase-γ (Polγ) catalytic subunit, is the most commonly mutated nuclear gene associated with mitochondrial disorders.

**Methods** We carried out whole-exome sequencing (WES) to identify the gene associated with progressive external ophthalmoplegia (PEO). We then performed histopathological analyses, assessed mitochondrial biology, and executed functional studies to evaluate the potential pathogenicity of the identified genetic mutations.

**Results** Novel biallelic *POLG* mutations, including a large deletion mutation (exons 7–21) and a missense variant c.1796C>T (p.Thr599Ile) were detected in the proband. Histopathological analysis of a biopsied muscle sample from this patient revealed the presence of approximately 20% COX-negative fibers. Bioinformatics analyses confirmed that the detected mutations were pathogenic. Furthermore, levels of mitochondrial complex I, II, and IV subunit protein expressions were found to be decreased in the proband, and marked impairment of mitochondrial respiration was evident in cells harboring these mutations.

**Conclusion** This study expands the spectrum of known *POLG* variants associated with PEO and advances current understanding regarding the structural and functional impacts of these mutations.

**Keywords** Mitochondrial disease · *POLG* · Large deletion · Missense variant · PEO

## Introduction

Mitochondrial disorders are clinically heterogeneous conditions associated with dysfunctional cellular energy production arising as a consequence of oxidative phosphorylation (OXPHOS) defects [1, 2]. These disorders can originate from mutated nuclear DNA (nDNA) or in maternally inherited mitochondrial DNA (mtDNA) [2, 3]. Over 1100 nDNA-encoded proteins are found in mitochondria, including OXPHOS subunits, assembly factors, and proteins related to other essential mitochondrial functions [4].

mtDNA polymerase γ (Polγ) is a key regulator of mtDNA replication and homeostasis [5–7]. Human Polγ is a heterotrimeric protein complex containing the catalytic 140-kDa POLG subunit encoded by *POLG* (MIM 174763) on chromosome 15q25 and the 55-kDa accessory subunit POLG2 encoded by *POLG2* (MIN 604983) on chromosome 17q24.1[7]. POLG possesses both 3′ → 5′ exonuclease activity and 5′ → 3′ polymerization activity. *POLG* genetic variants affect mtDNA stability and nucleotide metabolism, resulting in mtDNA defects including deletions, depletions, base-pair substitutions, and rearrangements, which can in turn give rise to mitochondrial diseases [5, 8, 9].

*POLG* is the nuclear gene that is most often mutated in the context of mitochondrial disorders. Van Goethem et al. first

Chuanzhu Yan and Kunqian Ji contributed equally to this work.

✉ Kunqian Ji
jikunqian@qq.com

✉ Chuanzhu Yan
czyan@sdu.edu.cn; chuanzhuyan@163.com

[1] Research Institute of Neuromuscular and Neurodegenerative Diseases and Department of Neurology, Qilu Hospital Cheeloo College of Medicine, Shandong University, No. 107 West Wenhua Road, Jinan 250012, Shandong, China

[2] Mitochondrial Medicine Laboratory, Qilu Hospital (Qingdao), Shandong University, Qingdao 266035, Shandong, China

[3] Brain Science Research Institute, Shandong University, Jinan 250012, Shandong, China

reported a *POLG* variant in a Belgian patient with progressive external ophthalmoplegia (PEO) in 2001 [10]. Since then, *POLG* has been the focus of intensive research. To date, there are approximately 300 related *POLG* variants have been documented (http://tools.niehs.nih. gov/polg/), the majority of which are point mutations, whereas *POLG* deletion mutations are extremely rare and have been identified only sporadically. *POLG* variant-related disorders are associated with a heterogeneous array of pathogenic mechanisms, clinical presentations, and outcomes. Neurological disorders may include devastating infantile disorders such as Alpers-Huttenlocher syndrome (AHS), mitochondrial recessive ataxia syndrome (MIRAS), myocerebrohepatopathy spectrum (MCHS), juvenile and adult-onset myoclonic epilepsy, ataxia neuropathy spectrum (ANS), sensory ataxia neuropathy dysarthria and ophthalmoplegia (SANDO), and mitochondrial neurogastrointestinal encephalopathy (MNGIE). Such variants can also cause late-onset disorders including myopathies such as PEO and certain movement disorder syndromes [5, 11–15].

PEO, which is the most prevalent form of mitochondrial myopathy, usually presents with progressive bilateral ptosis, diffuse symmetric ocular motility reductions, and exercise intolerance [16, 17]. Approximately half of all PEO cases originate from nDNA mutations in genes like *POLG*, *POLG2*, *SLC25A4*, *C10orf2*, *TWINKLE*, *PEO1*, *RRM2B*, *TK2*, or *OPA1* [16, 18–21]. The most prevalent *POLG* pathogenic variants include c.1399G>A (p.A467T) and c.2344G>C (p.W748S), which are closely related to autosomal-dominant (AD) and/or autosomal-recessive(AR) PEO [8, 22–24].

In our study, we report the case of a 33-year-old male with PEO harboring novel biallelic mutations in the *POLG* gene, including a large deletion mutation (exons 7–21) and a missense variant c.1796C>T (p.Thr599Ile). We confirmed the pathogenicity of these mutations based on a combination of clinical, genetical, and biochemical investigations.

## Materials and methods

### Subject

This 33-year-old male was the only child born to a non-consanguineous healthy couple. The patient first presented with strabismus and ptosis 9 months ago, accompanied by the gradual development of ophthalmoplegia. Aside from these ocular complaints, he did not report any other clinically relevant symptoms. The patient had no family history of known mitochondrial disease. A neurologic examination revealed bilateral ptosis, left exotropia (20 prism diopters), and ophthalmoparesis associated with mildly restricted eye movement. Reflexes, strength, and sensation examinations were all normal for this patient. Magnetic resonance imaging (MRI), electromyography (EMG), blood testing, and electroencephalography (EEG) findings were all normal. Informed consent for diagnosis and research studies was received from the patient. The study protocol was agreed upon the ethics committee of Qilu Hospital.

### Genomic analysis

After informed consent was provided, total genomic DNA was isolated from the peripheral blood and/or biopsied skeletal muscle samples from the proband and his parents using a DNA Isolation Kit (Blood DNA Kit V2, CW2553). Purification was then performed with Agencourt AMPure XP magnetic beads (Beckman Coulter), and targeted DNA samples were sequenced via whole-exome sequencing (WES) according to standard Illumina protocols using a Novaseq 6000 platform. The Burrows-Wheeler Alignment (BWA) Tool was used to align paired-end 200-bp reads to the human reference genome (hg19). Data were then collected and subjected to bioinformatics analyses, and candidate variants were analyzed based upon American College Medical Genetics and Genomics (ACMG) guidelines. Traditional Sanger sequencing was employed for the confirmation of the identified variants and to test the carrier status of clinically unaffected family members.

### mtDNA deletion analysis

DNA was obtained from muscle biopsies and peripheral blood samples from the proband according to standard protocols. The entire mitochondrial genome was screened via whole-exome sequencing (WES) and long-range polymerase chain reaction (PCR).

### Identification of pathogenic POLG variants

The pathogenicity of novel missense variants was assessed based on the following criteria: (1) the variants exhibited full disease phenotype co-segregation; (2) the involved amino acid residue was conserved; (3) the mutation was predicted to be associated with functional consequences according to analyses conducted using SIFT (http://www.sift.jcvi.org/), MutationTaster (http://www.mutationtaster.org), and PolyPhen (http://www.genetics. bwh.harvard.edu/pph/); (4) the affected amino acid was located in important functional domains; (5) a distinct disease-causing variant was known to exist at the same position; and (6) the variant was absent in 100 normal controls.

### Crystal structure determination

The structural impact of *POLG* variants was visualized and analyzed using the holoenzyme coordinate sets (pdb code:

5c53) and PyMOL (v2.0.6). A point variant model was produced using UCSF chimera. A large deletion predictive model was generated using the I-Tasser, Phyre2, and SWISS-MODEL programs [25–27].

### Histopathological examination

A left biceps brachii biopsy sample was taken from the proband, with serial 10-μm-thick cryosections being stained based on conventional histological protocols [28]. Staining approaches used were as follows: hematoxylin and eosin (H&E) staining, NADH-tetrazolium reductase staining, cytochrome *c* oxidase (COX) staining, modified Gomori trichrome (MGT) staining, succinate dehydrogenase (SDH) staining, and SDH-COX double staining following incubation at a pH of 4.3 and 10.4.

### Cell culture and cell line generation

Epstein-Barr Virus (EBV) was used to immortalize lymphoblastoid cell lines (LCLs) based upon a published protocol [29]. This approach was used to prepare cell lines from both the patient and age- and sex-matched healthy volunteers. All LCLs were grown using RPMI-1640 (Macgene), containing 10% fetal bovine serum (FBS, Gibco) and 0.11 mg/mL pyruvate (Macgene).

### Western blotting

Individual of 15–20 μg of protein samples retrieved from lysed muscle homogenates and LCLs were separated by SDS-PAGE and transferred to PVDF membranes (Millipore, USA), which were subsequently blocked for 1 h using a 5% non-fat milk solution, followed by overnight incubation at 4°C with a total OXPHOS human antibody cocktail (ab110411, Abcam), or with antibodies specific for ND4 (A9941, ABclonal), ND1 (ab181848, Abcam), ND5 (ab92624, Abcam), CYB (ab81215, Abcam), CO4 (4850s, CST), β-actin (ab8226, Abcam), or GAPDH (ab8245, Abcam). After that, secondary HRP-linked antibodies were used to detect primary antibodies (Beyotime A0216, A0208). An ECL system (Tanon 4600 SF) was then used to detect protein bands, with ImageJ being used for densitometric analyses.

### Oxygen consumption rate measurements

Cellular oxygen consumption rate (OCR) values were calculated using a Seahorse XFe24 instrument (Agilent, Santa Clara, CA, USA). Different respiratory chain inhibitors were introduced in sequence to analyze cellular respiration. LCLs were seeded at $3 \times 10^5$ cells/well on plates coated with a Cell-Tak™ adhesive (Corning) for 30 min. Cells were spun at 200×*g* for 1 min and were then incubated with culture medium for 30 min. The XFe24 cartridge was placed in calibration solution at 37°C for 12 h. For more details regarding these assay protocols, see prior studies [30].

### Mitochondrial stress test

Culture medium was replaced with assay medium (Cat# 103334-100, Seahorse Biosciences). Cells were then exposed to the inhibitors listed below: oligomycin A (1 μM), carbonyl cyanide 4-trifluoromethoxy-phenylhydrazone (FCCP, 0.5 μM), rotenone (1 μM), and antimycin A (1 μM). Assay medium and inhibitors were adjusted to a pH of 7.4 prior to use.

### Mitochondrial respiration assay

Culture medium was removed and mitochondrial assay solution (MAS) buffer (sucrose 70 mM, mannitol 210 mM, $KH_2PO_4$ 10 mM, $MgCl_2$ 5 mM, HEPES 2 mM, EDTA 1 mM, and BSA 0.2% (*w*/*v*)) was added in its place, while pyruvate (10 mM), malate (5 mM), and FCCP (0.5 μM) were used as buffer substrates. Digitonin (25 μg/ml, Sigma) was used to permeabilize cells. The injections were composed of rotenone (2 μM), succinate (10 mM), antimycin A (5 μM), ascorbate (10 mM), and *N*,*N*,*N*′,*N*′-tetramethyl-p-phenylenediamine (TMPD, 0.5 mM). All solutions and injections had a pH of 7.2.

### Statistical analysis

The presented data are given as means ± standard deviations (SDs). Normally distributed data were analyzed via independent two-sample *t*-tests or one-way ANOVAs as appropriate using SPSS 22.0 (IBM, IL, USA). $P < 0.05$ was the significance threshold for this study.

## Results

### Recognizing novel pathogenic POLG mutations

Using a WES approach, we identified two novel biallelic *POLG* mutations in the proband patient, including a large deletion mutation between exons 7 and 21 and a missense variant in exon 10 (c.1796C>T, p.Thr599Ile). To identify the breakpoints of the deleted allele, a PCR assay was then designed, and subsequent PCR product sequencing revealed a large 9223-bp deletion within *POLG* (chr15: 89,861,596-89,870,890). When this region was further analyzed via long-range PCR, the large intragenic deletion was confirmed de novo (Fig. 1D, E). The novel missense variant (c.1796C>T, p.T599I) was inherited from the proband's

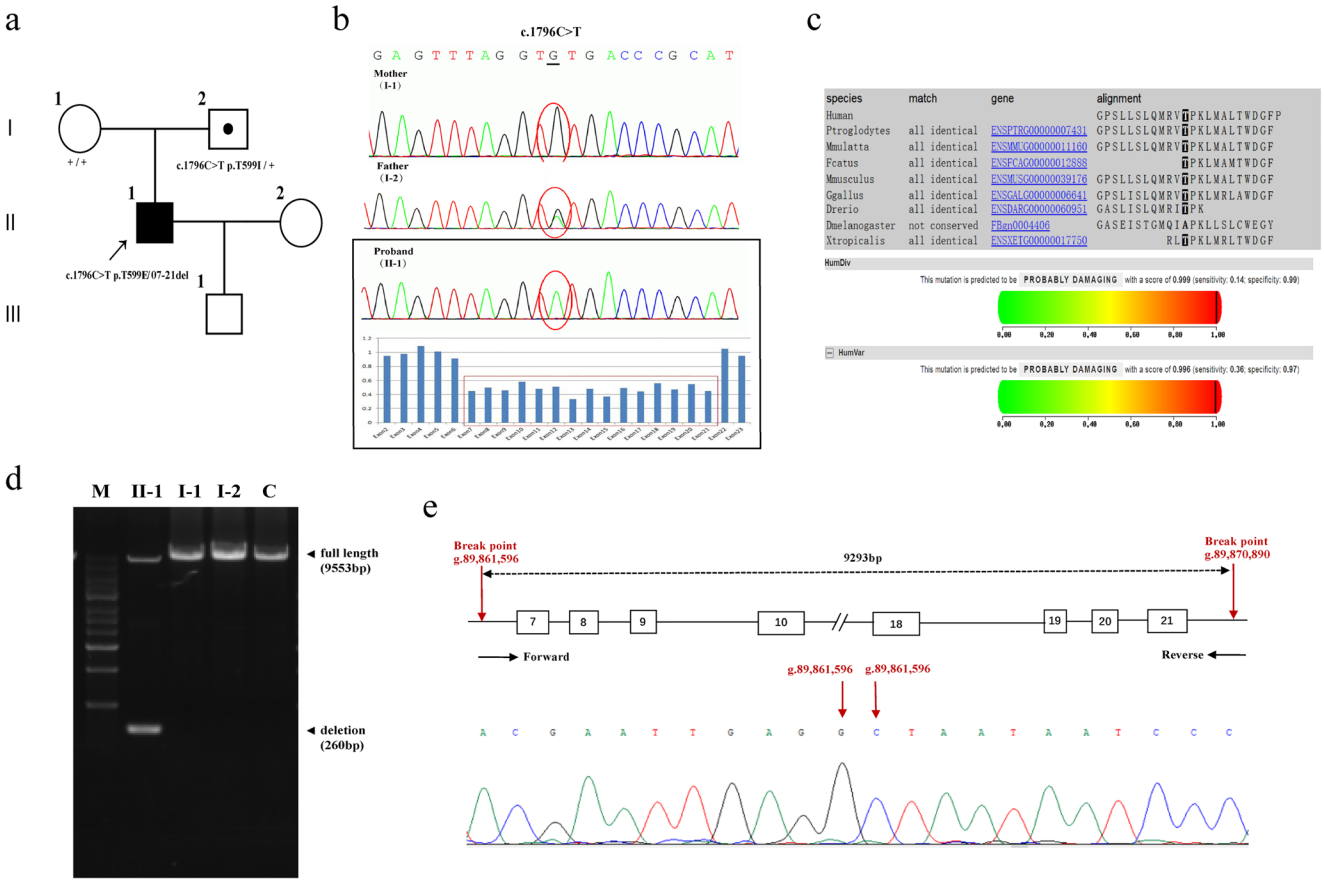


**Fig. 1** Analysis of novel biallelic mutations in the *POLG* gene. Family pedigree. The proband is indicated by an arrow. +/+, homozygous for the wild-type allele. E, exon; del, deletion. Genomic DNA sequencing revealed novel biallelic mutations in the *POLG* gene, including a missense variant (exon 10, c.1796C>T, p.Thr599Ile) inherited from the father, and a spontaneous large deletion mutation (E7–E21). Owing to the large deletion, the missense variant was homozygous in the proband. A multi-alignment analysis demonstrated that the affected amino acid residue was highly conserved among different species. The PolyPhen-2 predictive tool designated this mutation as being "probably damaging." Long-range PCR analysis of the *POLG* gene using primers located in introns 7 and 21. A full-length product (9553 bp) was detectable in the mother (I-1), the father (I-2), the patient (II-1), and a healthy control (C). However, a 260-bp deletion product was also detected in a heterozygous state in the patient (primers: forward 5′-gctaaggctgaagaaaataaatgtgt-3′ and reverse 5′-attttccaaatagaaaagcgtgagta-3′). M, molecular weight marker. Sequencing of the PCR deletion product identified the deletion breakpoints

father. There are no prior records of these two variants in the Human Gene Mutation Database (HGMD, www.hgmd.cf.ac.uk/) or on PubMed. A multi-alignment analysis further demonstrated that this missense variant modulated highly conserved amino acids. The PolyPhen-2 and Mutation Taster prediction programs further indicated that the c.1796C>T variant was damaging, while SIFT predicted this variant to be tolerated (Fig. 1B, C).

## The effect of the detected mutations on POLG structure

We assessed the impact of these biallelic mutations on the structure of Polγ. Interactive visualizations of this holoenzyme, which consists of the catalytic POLG subunit and the homodimeric POLG2 accessory subunit, were constructed using PyMOL. Predictive protein structural analyses of the large deletion in POLG were analyzed via three computational approaches. Despite the presence of the exonuclease domain in the mutant protein, the majority of the polymerase domain was removed by this deletion, and this mutation was predicted to be highly disruptive to the enzymatic functionality (Fig. 2A). Using the UCSF Chimera program, we next created a model of the T599I substitution. The hydrogen bond between threonine 599 and serine 593 was predicted to stabilize the linkage between the polymerase and spacer domain, as well as the binding of DNA to this enzyme. Relative to the wild-type enzyme, this mutant isoform exhibited significant structural changes. Based upon the structural position of T599 and its interactions with surrounding amino acids, we speculated that polymorphisms affecting residues 592, 593, 594, and 595 may also interfere with the structural stability of POLG (Fig. 2B).

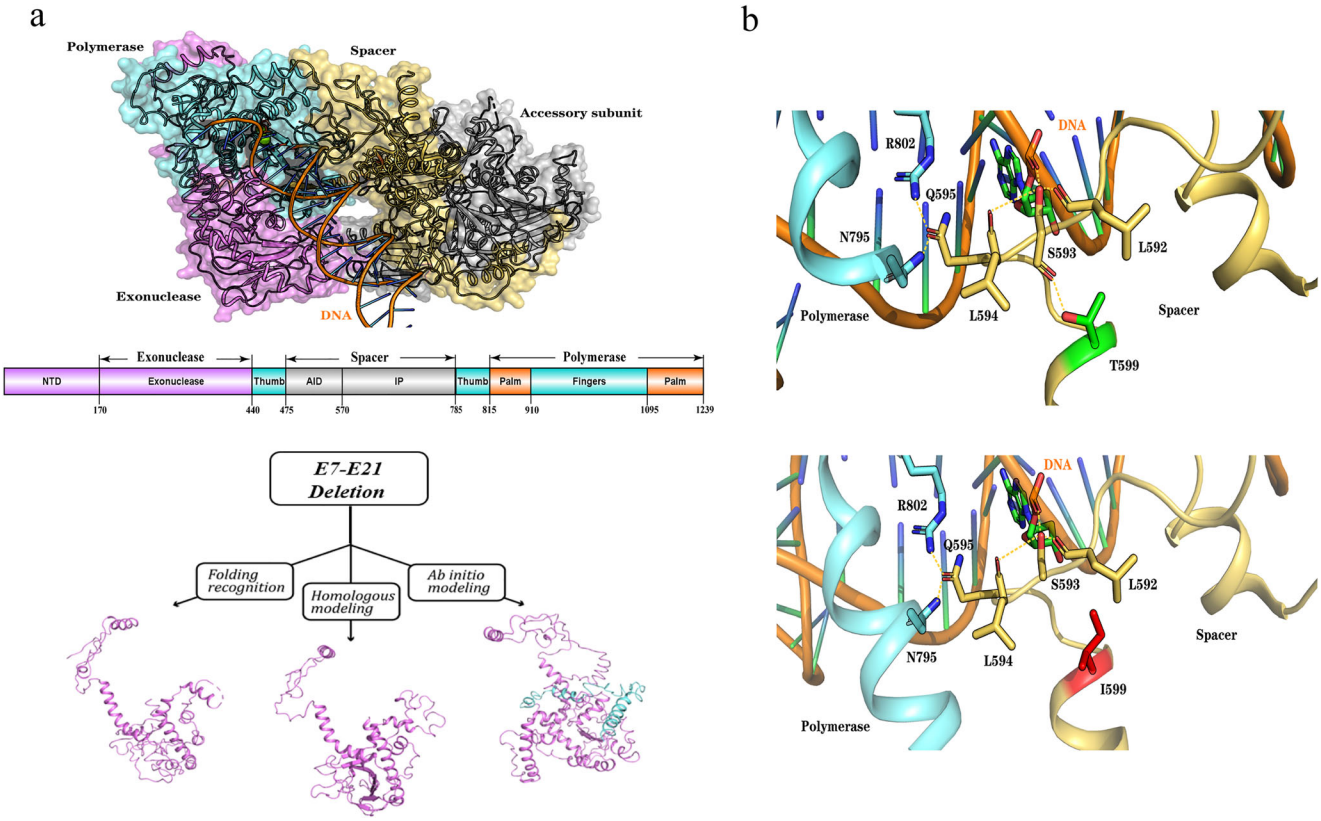


**Fig. 2** A three-dimensional schematic representation of the *POLG* large deletion mutation and T599I variant. *Upper panel*, the tertiary structure of the human Polγ holoenzyme [PDB code 5c53] with a DNA substrate. *Middle panel*, a schematic diagram of the human *POLG* gene. Surface domains are indicated as follows: exonuclease domain, purple; spacer domain, yellow; polymerase domain, blue; accessory subunit, gray. *Lower panel*, a prediction of the resultant protein stricter associated with the large E7–E21 deletion in *POLG*. The results were analyzed via three computational methods: fold recognition (using Phyre2), homologous modeling (using SWISS-MODEL), and ab initio modeling (using I-TASSER). Despite the remains of the exonuclease domain, the majority of the polymerase domain was deleted due to this mutation, and this was predicted to be highly disruptive to enzymatic function. *Upper panel*, Thr-599 is located in a loop in the spacer domain of POLG, close to the DNA substrate and the N terminal portion of the polymerase domain, and forms a hydrogen bond with the backbone of Ser-593, contributing to the stabilization of the local structure and its binding with DNA. *Lower panel*, the mutation of Thr-599 to Ile-599 mutations disrupts the hydrogen bond between amino acids 599 and 593, destabilizing the original hydrogen bonding framework and interfering with normal conformational transmission

## mtDNA deletion analysis

Deep mitochondrial genome sequencing conducted by NGS and long-range PCR amplification revealed the presence of a substantial mtDNA deletion (positions 5836-13922) in muscle samples but not blood samples from this patient, suggesting that the presence of mtDNA deletion is more common in postmitotic tissues in this genetic context (Supplementary Fig. 1).

## Histopathological analysis

Serial biceps brachii sections revealed pathological feature of typical mitochondrial disease. About 20% COX-negative fibers were observed upon MGT staining, with the majority being ragged red fibers (RRFs). SDH and S/C staining also revealed ragged blue fibers (RBFs) and blue-staining fibers, respectively, further supporting the diagnosis of mitochondrial disease (Fig. 3).

## Mitochondrial protein level reductions

To assess whether the identified variants affected OXPHOS subunit expression, we examined the levels of mtDNA-encoded respiratory complex subunits expression and the nDNA-encoded respiratory complex subunits expression in muscle tissues and LCLs via Western blot. GAPDH or β-actin were used as endogenous controls for these Western blotting assays. The levels of CO1 and nDNA-encoded NDUFB8 were strongly suppressed in the muscle tissue sample from this patient, where the nDNA-encoded SDHB expression was slightly reduced (Fig. 4A). Nine

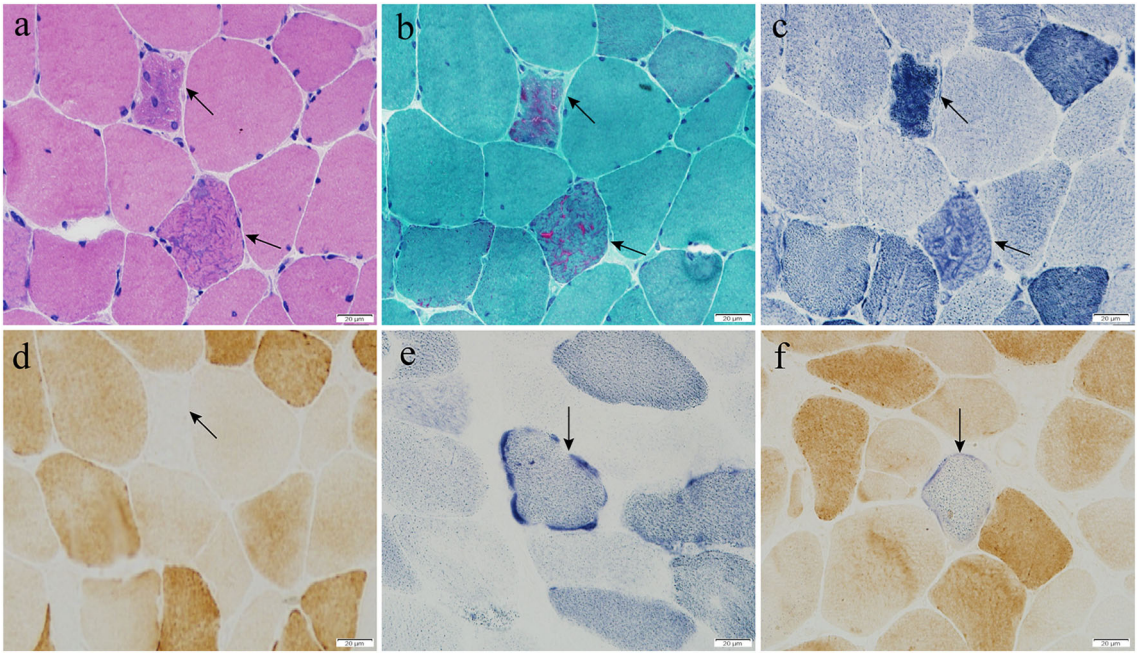


**Fig. 3** Histopathological characterization of the patient. **a** H&E staining revealed slight variability in muscle fiber size, with dark subsarcolemmal staining in several fibers. **b** MGT staining revealed numerous RRFs. **c** NADH staining revealed dark subsarcolemmal staining in several fibers. **d** COX staining revealed the presence of approximately 20% COX-negative fibers, some of which were RRFs. **e**, **f** RBFs and blue-stained fibers indicating reduced COX activity were detected via respective SDH and SDH-COX double staining. Arrows correspond to the indicated features. H&E, hematoxylin and eosin; MGT, modified Gomori trichrome; RRFs, ragged red fibers; NADH, nicotinamide adenine dinucleotide hydrate; COX, cytochrome *c* oxidase; SDH, succinate dehydrogenase; RBFs, ragged blue fibers

OXPHOS subunit expressions were reduced from 33.6 to 67.5% in mutant LCLs relative to control cells (Fig. 4B, C), while the expression of CYB and ATP5A in mutant LCLs was unchanged.

### Respiration deficiencies in mutant LCLs

In order to further investigate whether these identified variants modulated cellular bioenergetic activity, we next utilized a Seahorse XFe24 instrument to analyze control and mutant LCL respiratory functionality. Basal OCR in the resting state was reduced by 26.1% ($P = 0.013$) in mutant LCLs relative to control LCLs. We additionally employed electron transport chain (ETC) inhibitors or uncoupling agents to gauge the impact of the tested mutations on mitochondrial function in these cells. Relative to control cells, the ATP generation, proton leakage, maximum respiration, and spare capacity OCR values in mutant cells were lowered to 63.1% ($P = 0.012$), 72.3% ($P = 0.203$), 39.2% ($P = 0.001$), and 23.5% ($P < 0.001$), respectively (Fig. 5A, B). To elucidate the site-specific regulation of this variant on mitochondrial respiratory chain (MRC) activities, we examined complex I-, II-, and IV-mediated respiration in permeabilized LCLs. We discovered that mutant LCLs displayed marked reductions in all complex I-, II-, and IV-mediated respiration, as opposed to control LCLs (61.9%, 44.9%, and 83.7%, respectively) (Fig. 5C, D).

## Discussion

Herein, we described novel biallelic *POLG* mutations in a 33-year-old male with PEO, including a large deletion mutation (exons 7–21) and a missense variant c.1796C>T (p.Thr599Ile). Several lines of evidence suggested the pathogenicity of these novel biallelic mutations. First, this patient exhibited clinical symptoms and histological features consistent with adult-onset PEO. Second, these genetic defects co-segregated with the observed phenotype in the affected family. Third, large mtDNA deletions were identified in muscle samples from this patient. Fourth, these biallelic mutations resulted in reduced mitochondrial respiratory complex expression, with a particularly notable impact on the levels of complex I, II, and IV subunit expressions in the analyzed samples. Finally, LCLs carrying these variants exhibited marked mitochondrial dysfunction.

*POLG* is the nuclear gene that is most often found to be mutated in the context of mitochondrial disease [31]. Missense variants, accounting for 90% of reported *POLG* variants, are the most common form of such mutations. Deletion variants, however, are extremely rare, and have been identified only sporadically to date [5, 32]. In 2011, Tang et al. first reported a heterozygous large intragenic deletion (exons 15–21) with a common p.Ala467Thr variant in the *POLG* gene in an

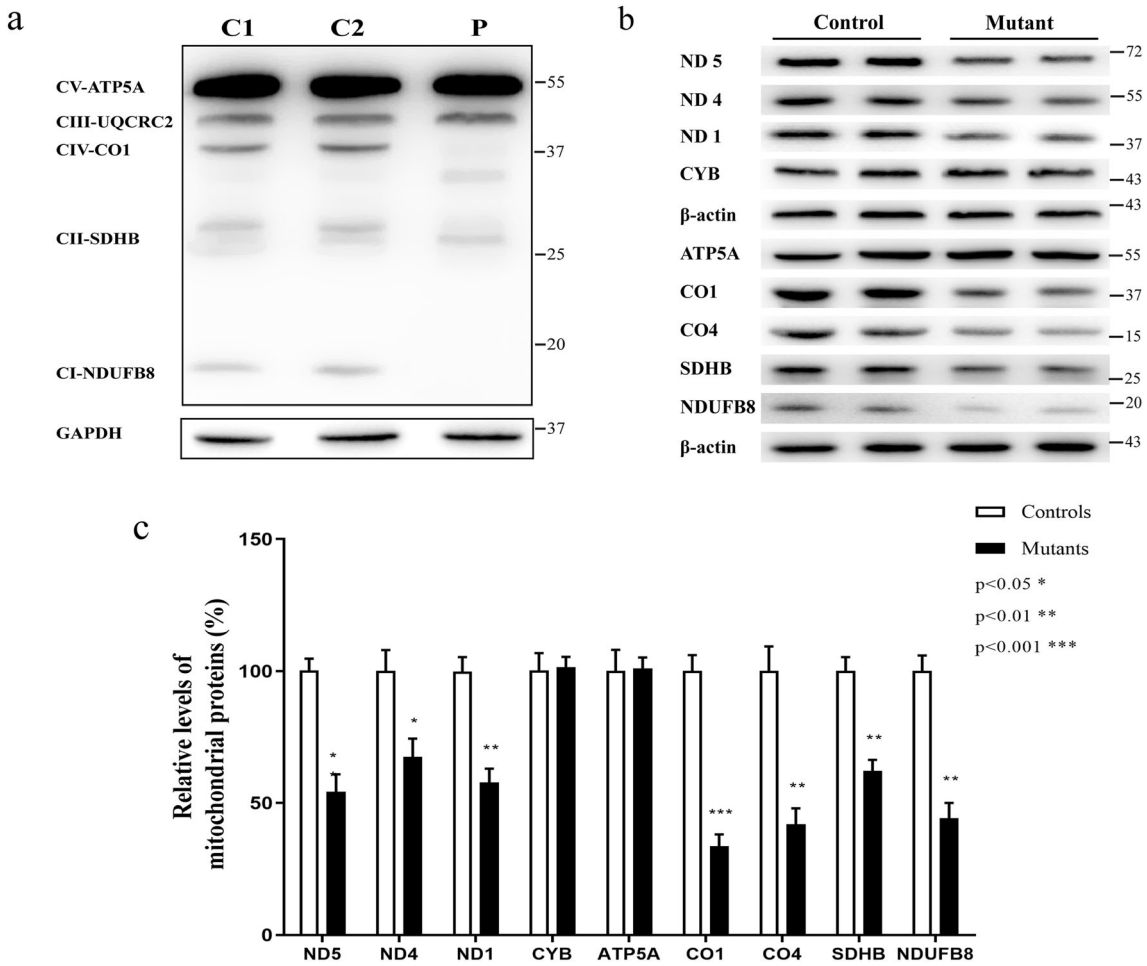


**Fig. 4** Western blotting analysis of mitochondrial proteins. An analysis of five OXPHOS subunits encoded by the mitochondrial and nuclear genes. In total, 5 μg of total protein from the muscle tissue of the patient (P) and controls (C) was analyzed. GAPDH was used as a loading control. Analysis of five mtDNA-encoded subunits (ND1, ND4, ND5, CYB, CO1) and four nDNA-encoded subunits (ATP5A, CO4, SDHB, and NDUFB8). In total, 20 μg samples of protein from mutant and control LCLs were analyzed. β-Actin was used as a loading control. The average levels of mitochondrial protein levels in mutant LCLs were compared to those in the control group. Values are from three separate experiments

Alpers syndrome patient [33]. In 2014, Rouzier et al. demonstrated the presence of a heterozygous large intragenic deletion mutation (intron 21–exon 22) and a p.Trp748Ser mutation in a child with refractory epilepsia partialis continua [34]. According to the ACMG guidelines for the classification of sequence variants, large deletions are deleterious and thus represent the best candidates for pathogenic variants [35]. The case reported in the present study was the third patient found to harbor large deletion mutation in the *POLG* gene to date.

We assessed the pathogenicity of the novel p.T599I variant. First, this variant fully co-segregated with the observed disease phenotype. The affected amino acid residue was highly conserved across various species, and the PolyPhen and MutationTaster predictive tools designated this variant as being damaging. Second, the threonine at position 599 is a crucial residue important for binding to upstream DNA. Using the PyMOL software, we found that the mutation of Thr-599 to Ile-599 disrupts hydrogen bond formation between residues 599 and 593, leading to the instability of the original hydrogen bonding framework and interfering with normal conformational transmission. Third, the novel T599I missense variant affected a highly conserved residue in the spacer domain. The spacer domain influences the conformation of the wall of the DNA-binding domain and is located between the exonuclease and polymerase domains where it is connected by the thumb subdomains [36]. Using the PyMOL and UCSF chimera programs, we found that the T599I variant blocks the DNA-binding channel and results in decreased DNA-binding affinity.

Most disease-causing missense variants in *POLG* are known to be associated with three common variations: p.A467T, p.W748S, and p.G848S [22, 23, 37–40]. The

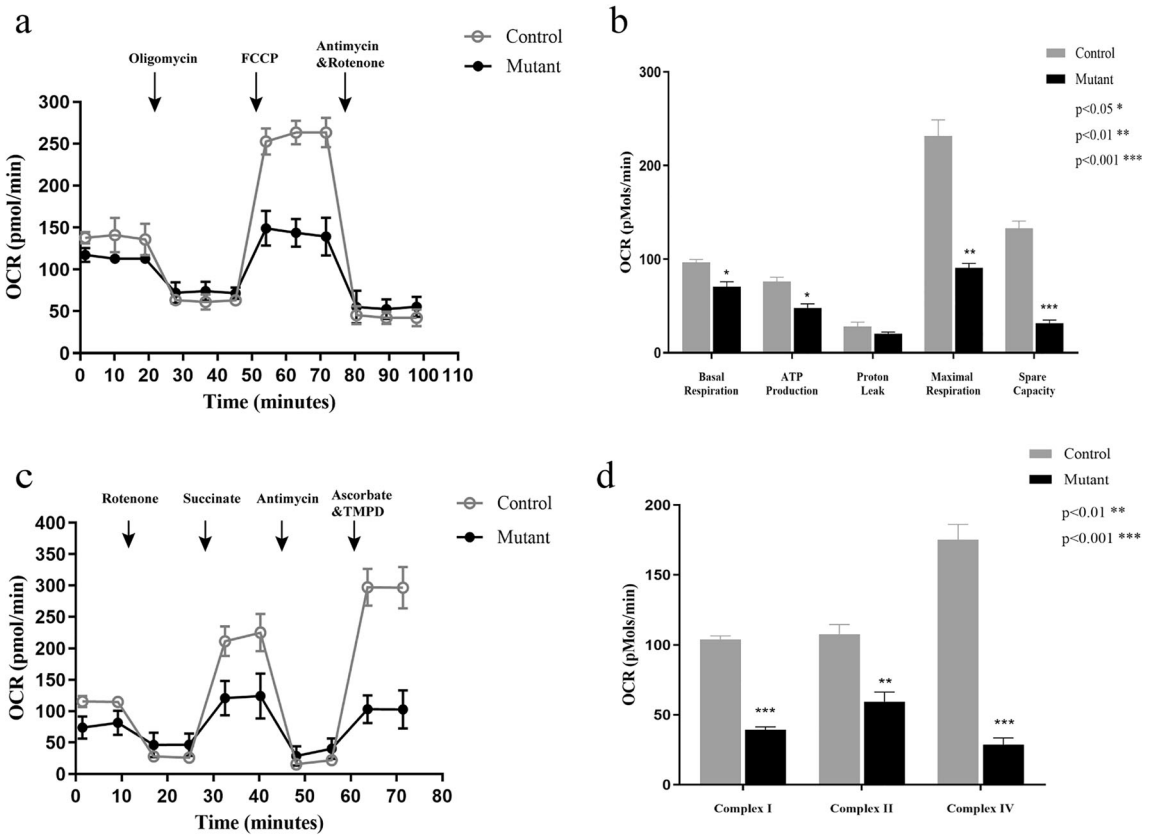


**Fig. 5** Cellular respiration analysis. Analysis of OCR in the mutant and control LCLs treated with different inhibitors. Bar graphs indicating basal respiration OCR, ATP production OCR, proton leak OCR, maximal respiration OCR, and spare capacity OCR. Data were compared via a two-sample *t*-test. $*P < 0.05$; $**P < 0.05$; $***P < 0.001$. Analysis of complex I-, II- and IV-mediated respiratory activity in mutant and control LCLs following the injection of the indicated compounds. Bar graphs indicating complex I-, II-, and IV-mediated respiratory activity. Data were compared via a two-sample *t*-test. $*P < 0.05$; $**P < 0.05$; $***P < 0.001$. OCR, oxygen consumption rate; LCLs, lymphoblastoid cell lines

A467T mutation is detected in roughly 36% of all POLG disease alleles, and it prevents the interaction between the POLG and POLG2 subunits, adversely impacting DNA synthesis and Polγ activity [38]. The W748S variant is the second most commonly documented POLG mutation in the POLG mutation database, exhibiting low-affinity DNA-binding activity and processivity but normal POLG2 interactions [39]. The G848S mutation is the third-most frequently detected POLG mutation and causes severely reduced DNA polymerase activity [40].

In conclusion, we described novel biallelic *POLG* mutations, including a large deletion (exons 7–21) mutation and a missense variant c.1796C>T (p.T599I), which were associated with a clinical presentation of PEO in a 33-year-old male. Biochemical investigations demonstrated that these variants severely impaired mitochondrial function, thereby leading to mitochondrial disease. Our study expands the spectrum of *POLG* variants known to cause PEO, offering valuable new insights into *POLG* variants with respect to both their structural and functional consequences.

**Supplementary Information** The online version contains supplementary material available at https://doi.org/10.1007/s10072-021-05380-2.

**Acknowledgements** The authors thank the proband and his family for giving consent, samples, and additional information for this study.

**Author contribution** Yan Lin: writing original draft. Jixiang Du and Wei Wang: data curation and assisted genetic testing. Hong Ren and Dandan Zhao: methodology and validation. Yuying Zhao, Pengfei Lin, and Fuchen Liu: supervision. Kunqian Ji and Chuanzhu Yan: review the final manuscript.

**Funding** This study was supported by the National Natural Science Foundation of China (No. 81701237 and 81671235), People's Benefit Project of Science and Technology in Qingdao (16-6-2-1-nsh), Collaborative Innovation and Achievement Transformation in Universities and Research Institutes of Jinan (2019GXRC050), Qingdao Key Health Discipline Development Fund, and the Taishan Scholars Program of Shandong Province.

**Data availabilty** The data that support the findings of this study are available from the corresponding author upon reasonable request.

## Declarations

**Conflict of interest** The authors declare no conflict of interest.

**Ethical approval** The study was approved by the Research Ethics Board of Qilu Hospital.

**Informed consent** We obtained all appropriate patient consent forms.

## References


1. Lightowlers RN, Taylor RW, Turnbull DM (2015) Mutations causing mitochondrial disease: what is new and what challenges remain? Science 349(6255):1494–1499. https://doi.org/10.1126/science.aac7516
2. Gorman GS, Schaefer AM, Ng Y, Gomez N, Blakely EL, Alston CL, Feeney C, Horvath R, Yu-Wai-Man P, Chinnery PF, Taylor RW, Turnbull DM, McFarland R (2015) Prevalence of nuclear and mitochondrial DNA mutations related to adult mitochondrial disease. Ann Neurol 77(5):753–759. https://doi.org/10.1002/ana.24362
3. Wong LJ, Boles RG (2005) Mitochondrial DNA analysis in clinical laboratory diagnostics. Clin Chim Acta 354:1–20. https://doi.org/10.1016/j.cccn.2004.11.003
4. Calvo SE, Clauser KR, Mootha VK (2016) MitoCarta2.0: an updated inventory of mammalian mitochondrial proteins. Nucleic Acids Res 44:D1251–D1257. https://doi.org/10.1093/nar/gkv1003
5. Rahman S, Copeland WC (2019) POLG-related disorders and their neurological manifestations. Nat Rev Neurol 15(1):40–52. https://doi.org/10.1038/s41582-018-0101-0
6. Roos S, Macao B, Fusté JM, Lindberg C, Jemt E, Holme E, Moslemi AR, Oldfors A, Falkenberg M (2013) Subnormal levels of POLγA cause inefficient initiation of light-strand DNA synthesis and lead to mitochondrial DNA deletions and progressive external ophthalmoplegia [corrected]. Hum Mol Genet 22(12):2411–2422. https://doi.org/10.1093/hmg/ddt094
7. Anderson AP, Luo X, Russell W, Yin YW (2020) Oxidative damage diminishes mitochondrial DNA polymerase replication fidelity. Nucleic Acids Res 48(2):817–829. https://doi.org/10.1093/nar/gkz1018
8. Milone M, Benarroch EE, Wong LJ (2011) POLG-related disorders: defects of the nuclear and mitochondrial genome interaction. Neurology 77(20):1847–1852. https://doi.org/10.1212/WNL.0b013e318238863a
9. Gaudó P, Emperador S, Garrido-Pérez N, Ruiz-Pesini E, Yubero D, García-Cazorla A, Artuch R, Montoya J, Bayona-Bafaluy MP (2020) Infectious stress triggers a POLG-related mitochondrial disease. Neurogenetics 21(1):19–27. https://doi.org/10.1007/s10048-019-00593-2
10. Van Goethem G, Dermaut B, Löfgren A, Martin JJ, Van Broeckhoven C (2001) Mutation of POLG is associated with progressive external ophthalmoplegia characterized by mtDNA deletions. Nat Genet 28(3):211–212. https://doi.org/10.1038/90034
11. Krasich R, Copeland WC (2017) DNA polymerases in the mitochondria: a critical review of the evidence. Front Biosci 22:692–709. https://doi.org/10.2741/4510
12. Hedberg-Oldfors C, Macao B, Basu S, Lindberg C, Peter B, Erdinc D, Uhler JP, Larsson E, Falkenberg M, Oldfors A (2020) Deep sequencing of mitochondrial DNA and characterization of a novel POLG mutation in a patient with arPEO. Neurol Genet 6(1):e391. https://doi.org/10.1212/nxg.0000000000000391
13. Fuke S, Kametani M, Yamada K, Kasahara T, Kubota-Sakashita M, Kujoth GC, Prolla TA, Hitoshi S, Kato T (2014) Heterozygous Polg mutation causes motor dysfunction due to mtDNA deletions. Ann Clin Transl Neurol 1(11):909–920. https://doi.org/10.1002/acn3.133
14. Da Pozzo P, Cardaioli E, Rubegni A, Gallus GN, Malandrini A, Rufa A, Battisti C, Carluccio MA, Rocchi R, Giannini F, Bianchi A, Mancuso M, Siciliano G, Dotti MT, Federico A (2017) Novel POLG mutations and variable clinical phenotypes in 13 Italian patients. Neurol Sci 38(4):563–570. https://doi.org/10.1007/s10072-016-2734-3
15. Finsterer J, Scorza FA (2018) Phenotypic spectrum of POLG1 mutations. Neurol Sci 39(3):571–573. https://doi.org/10.1007/s10072-017-3116-1
16. Heighton JN, Brady LI, Sadikovic B, Bulman DE, Tarnopolsky MA (2019) Genotypes of chronic progressive external ophthalmoplegia in a large adult-onset cohort. Mitochondrion 49:227–231. https://doi.org/10.1016/j.mito.2019.09.002
17. Rodríguez-López C, García-Cárdaba LM, Blázquez A, Serrano-Lorenzo P, Gutiérrez-Gutiérrez G, San Millán-Tejado B, Muelas N, Hernández-Laín A, Vílchez JJ, Gutiérrez-Rivas E, Arenas J, Martín MA, Domínguez-González C (2020) Clinical, pathological and genetic spectrum in 89 cases of mitochondrial progressive external ophthalmoplegia. J Med Genet 57(9):643–646. https://doi.org/10.1136/jmedgenet-2019-106649
18. Sommerville EW, Chinnery PF, Gorman GS, Taylor RW (2014) Adult-onset Mendelian PEO Associated with Mitochondrial Disease. J Neuromuscul Dis 1(2):119–133 doi:undefined
19. Milone M, Brunetti-Pierri N, Tang LY, Kumar N, Mezei MM, Josephs K, Powell S, Simpson E, Wong LJ (2008) Sensory ataxic neuropathy with ophthalmoparesis caused by POLG mutations. Neuromuscul Disord 18(8):626–632. https://doi.org/10.1016/j.nmd.2008.05.009
20. Ji K, Liu K, Lin P, Wen B, Luo YB, Zhao Y, Yan C (2014) Twinkle mutations in two Chinese families with autosomal dominant progressive external ophthalmoplegia. Neurol Sci 35(3):443–448. https://doi.org/10.1007/s10072-013-1557-8
21. Da Pozzo P, Rubegni A, Rufa A, Cardaioli E, Taglia I, Gallus GN, Malandrini A, Federico A (2015) Sporadic PEO caused by a novel POLG variation and a Twinkle mutation: digenic inheritance? Neurol Sci 36(9):1713–1715. https://doi.org/10.1007/s10072-015-2247-5
22. Neeve VC, Samuels DC, Bindoff LA, van den Bosch B, Van Goethem G, Smeets H, Lombès A, Jardel C, Hirano M, Dimauro S, De Vries M, Smeitink J, Smits BW, de Coo IF, Saft C, Klopstock T, Keiling BC, Czermin B, Abicht A, Lochmülle H, Hudson G, Gorman GG, Turnbull DM, Taylor RW, Holinski-Feder E, Chinnery PF, Horvath R (2012) What is influencing the phenotype of the common homozygous polymerase-γ mutation p.Ala467Thr? Brain 135:3614–3626. https://doi.org/10.1093/brain/aws298
23. Horvath R, Hudson G, Ferrari G, Fütterer N, Ahola S, Lamantea E, Prokisch H, Lochmüller H, McFarland R, Ramesh V, Klopstock T, Freisinger P, Salvi F, Mayr JA, Santer R, Tesarova M, Zeman J, Udd B, Taylor RW, Turnbull D, Hanna M, Fialho D, Suomalainen A, Zeviani M, Chinnery PF (2006) Phenotypic spectrum associated with mutations of the mitochondrial polymerase gamma gene. Brain 129:1674–1684. https://doi.org/10.1093/brain/awl088
24. Kollberg G, Moslemi AR, Darin N, Nennesmo I, Bjarnadottir I, Uvebrant P, Holme E, Melberg A, Tulinius M, Oldfors A (2006) POLG1 mutations associated with progressive encephalopathy in childhood. J Neuropathol Exp Neurol 65(8):758–768. https://doi.org/10.1097/01.jnen.0000229987.17548.6e

25. Yang J, Yan R, Roy A, Xu D, Poisson J, Zhang Y (2015) The I-TASSER Suite: protein structure and function prediction. Nat Methods 12(1):7–8. https://doi.org/10.1038/nmeth.3213
26. Kelley LA, Mezulis S, Yates CM, Wass MN, Sternberg MJ (2015) The Phyre2 web portal for protein modeling, prediction and analysis. Nat Protoc 10(6):845–858. https://doi.org/10.1038/nprot.2015.053
27. Waterhouse A, Bertoni M, Bienert S, Studer G, Tauriello G, Gumienny R, Heer FT, de Beer TAP, Rempfer C, Bordoli L, Lepore R, Schwede T (2018) SWISS-MODEL: homology modelling of protein structures and complexes. Nucleic Acids Res 46:W296–W303. https://doi.org/10.1093/nar/gky427
28. Dubowitz V, Sewry CA, Oldfors A (2013) Muscle biopsy. A Practical Approach, 4th edn. Elsevier, Philadelphia, pp 1–592
29. Miller G, Lipman M (1973) Release of infectious Epstein-Barr virus by transformed marmoset leukocytes. Proc Natl Acad Sci U S A 70(1):190–194. https://doi.org/10.1073/pnas.70.1.190
30. van der Windt GJW, Changm CH, Pearce EL (2016) Measuring bioenergetics in T cells using a seahorse extracellular flux analyzer. Curr Protoc Immunol 113(3):16B.11-13–16B16B.14. https://doi.org/10.1002/0471142735.im0316bs113
31. Stumpf JD, Copeland WC (2011) Mitochondrial DNA replication and disease: insights from DNA polymerase γ mutations. Cell Mol Life Sci 68(2):219–233. https://doi.org/10.1007/s00018-010-0530-4
32. Nissanka N, Bacman SR, Plastini MJ, Moraes CT (2018) The mitochondrial DNA polymerase gamma degrades linear DNA fragments precluding the formation of deletions. Nat Commun 9(1):2491. https://doi.org/10.1038/s41467-018-04895-1
33. Tang S, Wang J, Lee NC, Milone M, Halberg MC, Schmitt ES, Craigen WJ, Zhang W, Wong LJ (2011) Mitochondrial DNA polymerase gamma mutations: an ever expanding molecular and clinical spectrum. J Med Genet 48(10):669–681. https://doi.org/10.1136/jmedgenet-2011-100222
34. Rouzier C, Chaussenot A, Serre V, Fragaki K, Bannwarth S, Ait-El-Mkadem S, Attarian S, Kaphan E, Cano A, Delmont E, Sacconi S, Mousson de Camaret B, Rio M, Lebre AS, Jardel C, Deschamps R, Richelme C, Pouget J, Chabrol B, Paquis-Flucklinger V (2014) Quantitative multiplex PCR of short fluorescent fragments for the detection of large intragenic POLG rearrangements in a large French cohort. Eur J Hum Genet 22(4):542–550. https://doi.org/10.1038/ejhg.2013.171
35. Richards CS, Bale S, Bellissimo DB, Das S, Grody WW, Hegde MR, Lyon E, Ward BE (2008) ACMG recommendations for standards for interpretation and reporting of sequence variations: Revisions 2007. Genet Med 10(4):294–300. https://doi.org/10.1097/GIM.0b013e31816b5cae
36. Euro L, Farnum GA, Palin E, Suomalainen A, Kaguni LS (2011) Clustering of Alpers disease mutations and catalytic defects in biochemical variants reveal new features of molecular mechanism of the human mitochondrial replicase, Pol γ. Nucleic Acids Res 39(21):9072–9084. https://doi.org/10.1093/nar/gkr618
37. Craig K, Ferrari G, Tiangyou W, Hudson G, Gellera C, Zeviani M, Chinnery PF (2007) The A467T and W748S POLG substitutions are a rare cause of adult-onset ataxia in Europe. Brain 130:E69; author reply–E70. https://doi.org/10.1093/brain/awm009
38. Wong LJ, Naviaux RK, Brunetti-Pierri N, Zhang Q, Schmitt ES, Truong C, Milone M, Cohen BH, Wical B, Ganesh J, Basinger AA, Burton BK, Swoboda K, Gilbert DL, Vanderver A, Saneto RP, Maranda B, Arnold G, Abdenur JE, Waters PJ, Copeland WC (2008) Molecular and clinical genetics of mitochondrial diseases due to POLG mutations. Hum Mutat 29(9):E150–E172. https://doi.org/10.1002/humu.20824
39. Hakonen AH, Heiskanen S, Juvonen V, Lappalainen I, Luoma PT, Rantamaki M, Goethem GV, Lofgren A, Hackman P, Paetau A, Kaakkola S, Majamaa K, Varilo T, Udd B, Kaariainen H, Bindoff LA, Suomalainen A (2005) Mitochondrial DNA polymerase W748S mutation: a common cause of autosomal recessive ataxia with ancient European origin. Am J Hum Genet 77(3):430–441. https://doi.org/10.1086/444548
40. Kasiviswanathan R, Longley MJ, Chan SS, Copeland WC (2009) Disease mutations in the human mitochondrial DNA polymerase thumb subdomain impart severe defects in mitochondrial DNA replication. J Biol Chem 284(29):19501–19510. https://doi.org/10.1074/jbc.M109.011940